Nucleic Acids Research, 2012, **1–10**
doi:10.1093/nar/gks817

Protein-induced changes in DNA structure and dynamics observed with noncovalent site-directed spin labeling and PELDOR

Gunnar W. Reginsson[1,2], Sandip A. Shelke[2], Christophe Rouillon[3], Malcolm F. White[3], Snorri Th. Sigurdsson[2] and Olav Schiemann[1,*]

[1]Biomedical Sciences Research Complex, Centre of Magnetic Resonance, University of St Andrews, St Andrews KY16 9ST, UK, [2]Science Institute, University of Iceland, Dunhaga 3, 107 Reykjavík, Iceland and [3]Biomedical Sciences Research Complex, University of St Andrews, St Andrews KY16 9ST, UK

Received May 7, 2012; Revised July 23, 2012; Accepted August 5, 2012

ABSTRACT

Site-directed spin labeling and pulsed electron–electron double resonance (PELDOR or DEER) have previously been applied successfully to study the structure and dynamics of nucleic acids. Spin labeling nucleic acids at specific sites requires the covalent attachment of spin labels, which involves rather complicated and laborious chemical synthesis. Here, we use a noncovalent label strategy that bypasses the covalent labeling chemistry and show that the binding specificity and efficiency are large enough to enable PELDOR or DEER measurements in DNA duplexes and a DNA duplex bound to the Lac repressor protein. In addition, the rigidity of the label not only allows resolution of the structure and dynamics of oligonucleotides but also the determination of label orientation and protein-induced conformational changes. The results prove that this labeling strategy in combination with PELDOR has a great potential for studying both structure and dynamics of oligonucleotides and their complexes with various ligands.

INTRODUCTION

Nucleic acids play a complex role in biological processes. Therefore, it is of great importance to solve their structure and conformational distribution to understand the structure–function relationship of nucleic acids or nucleic acid/protein complexes. Pulsed electron–electron double resonance (PELDOR or DEER) (1,2), together with site-directed spin labeling (SDSL) (3,4), is increasingly being used as a method for structure determination of biomolecules (5). PELDOR is a pulsed electron paramagnetic resonance (EPR) technique that is capable of measuring distances in the range of 2–8 nm between spin centers in biological samples (6). Therefore, this method requires that the nucleic acids be labeled with molecules that carry an unpaired electron, the so-called spin labels.

The most widely used family of spin labels is nitroxides (7). These labels can be attached to the sugar, base or phosphate backbone via linkers of different flexibilities, either during chemical synthesis of the nucleic acid or postsynthetically (3,5). Since flexible linkers introduce an unwanted distribution to distance measurements, the determination of precise distances and conformational distribution of nucleic acid becomes more challenging. A way to get around this problem is incorporating rigid spin labels (8,9). The rigid spin label **Ç** (Figure 1a), reported by Sigurdsson *et al.* (9–11), has afforded precise distance measurements, mutual orientation of spin labels and conformational dynamics of nucleic acids through EPR (9, 12–14). However, all of these labeling strategies require covalent attachment of the label and, thus, rather elaborate organic synthesis, which hampers the wide application and dissemination of this technique.

Recently, we have developed a noncovalent SDSL strategy (NC-SDSL) that utilizes spin label **ç** (15), the nucleobase of the rigid spin label nucleoside **Ç**. Spin label **ç** binds to the abasic site in duplex DNA by hydrogen bonding with the orphan guanine (G) base present on the complementary strand and by stacking interaction with base pairs flanking the abasic site. Since the DNAs that contains abasic sites are commercially available, the preparation of spin-labeled nucleic acid sample has become as simple as mixing a spin label with a duplex DNA containing abasic sites. Here, we show that

*To whom correspondence should be addressed. Tel: +44 1334 463410; Fax: +44 1334 462595; Email: os11@st-andrews.ac.uk
Present address:
Olav Schiemann, Institute of Physical and Theoretical Chemistry, University of Bonn, Bonn 53115, Germany.

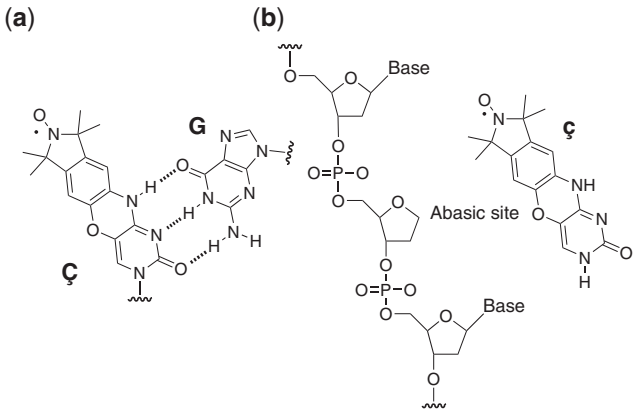

Figure 1. Structures of spin labels and abasic site. (**a**) The rigid spin label **Ç** base paired with G. (**b**) A DNA oligomer containing an abasic site and the rigid spin label ç.

the specificity and binding efficiency of **ç** for abasic sites in duplex DNAs (Table 1) are high enough to permit PELDOR measurements with resolved modulations and orientation selectivity. Furthermore, we show on the DNA/Lac repressor system that such measurements can be performed in the presence of DNA-binding proteins and that they enable one to observe DNA bending and dynamics.

MATERIALS AND METHODS

General procedures

NaCl and 2-(*N*-morpholino)ethanesulfonic acid (MES) were obtained from Fluka. $Na_2HPO_4 \cdot 6\ H_2O$, ethanol and ethylenediaminetetraacetic acid (EDTA) were obtained from Fischer Scientific. Ethylene glycol was obtained from Aldrich. Deuterated ethylene glycol (98%) and deuterium oxide (99%) were obtained from Cambridge Isotope Laboratories.

Synthesis and purification of DNA oligomers

29-Mer Ç labeled DNA oligomers were synthesized and purified as previously reported (11)

DNA oligomers containing abasic sites were synthesized by a trityl-off synthesis on a 1.0 µmol scale (1000 Å CPG columns) using an automated ASM 800 Biosset DNA synthesizer and phosphoramidites with standard protecting groups. 1,2-Dideoxy D-ribose CED phosphoramidite was used as a building block for abasic oligomer synthesis. The DNA oligomers were deprotected in concentrated ammonia solution at 55°C for 8 h and purified by 20% denaturing polyacrylamide gel electrophoreses (DPAGE). The oligonucleotides were visualized by ultraviolet (UV) shadowing, and the bands excised from the gel were crushed and soaked in TEN buffer (10 mM Tris pH 7.5, 250 nM NaCl and 1 mM Na_2EDTA). The DNA elution solutions were filtered through a 0.45-µm polyethersulfone membrane (disposable filter device from Whatman) and desalted using Sep-Pak cartridge (Waters Corporation) according to manufacturer's instructions. After removing the solvent under vacuum, the oligonucleotides were dissolved in deionized and sterilized water (200 µl). All commercial phosphoramidites, CPG columns and solutions for DNA synthesis were purchased from ChemGenes Corporation.

29-Mer DNA oligomers containing 19-mer LacI operator sequence and abasic sites were purchased from Eurogentec. Purification was done with DPAGE and quality control by MALDI-TOF mass spectrometry.

The concentration of DNA oligomers was calculated from Beer's law based on measurements of absorbance at 260 nm, using a 50 Bio UV–visible spectrometer from Varian, equipped with a 100 µl cell (optical path length = 1 cm). Extinction coefficients of DNA oligomers were determined using the UV WinLab oligonucleotide calculator (V2.85.04, Perkin Elmer). ssDNA oligomers solutions (1 µl) were dissolved in sterilized water (99 µl) and transferred to spectrometer cell for measurements. Sterilized water was used as a reference sample. Evaporation of solvents under vacuum was carried out on an SPD 111-V speed-vac from Savant equipped with vapor trap and vacuum inversion. Preparation of all DNA samples for EPR measurements were done in sterile Biopur Eppendorf tubes (2 ml) with cap.

Hybridization of oligonucleotides

Hybridization of all DNA oligomers was performed with a PCH-2 heating block from Grant-bio. Complementary DNA strands were annealed according to the following program: 90°C for 2 min, 60°C for 5 min, 50°C for 5 min, 40°C for 5 min, 22°C for 15 min. The DNA samples were stored at −30°C.

Preparation of dsDNA 1

Synthesized and purified DNA oligomers were reconstituted with sterile water in Biopur Eppendorf tubes (2 ml). Noncovalently spin-labeled DNA duplexes were prepared by mixing appropriate single-stranded DNA oligomers (5 nmol) with two equivalents of spin label **ç** dissolved in ethanol (10 nmol). The water/ethanol solution was evaporated under vacuum and the dry sample was dissolved in phosphate buffer (Na_2HPO_4 10 mM, NaCl 100 mM, Na_2EDTA 0.1 mM, pH 7.00) (100 µl). After annealing the DNA oligomers, the solvent was removed under vacuum. The dry sample was dissolved in sterile water with 20% (v/v) ethylene glycol (100 µl). All samples were transferred to a quartz EPR tube, rapidly frozen in (1:4 methylcyclohexane:iso-pentane at −165°C) and stored in liquid nitrogen.

Preparation of dsDNA 2

29-Mer DNA oligomers (4 nmol) were mixed with two equivalents of **ç** dissolved in ethanol (8 nmol) and annealed in phosphate buffer (Na_2HPO_4 10 mM, NaCl 100 mM, Na_2EDTA 0.1 mM, pH 7.00) (100 µl). The solvent was removed under vacuum, and the dry sample was dissolved in MES buffer (MES 20 mM pH 6.0, NaCl 300 mM, in ^2H_2O) (80 µl) and deuterated ethylene glycol (20 µl). The sample was transferred to an EPR tube, rapidly frozen in a freezing mixture and stored in liquid nitrogen.

Table 1. Sequences for the dsDNAs containing abasic sites that were noncovalently spin labeled

DNA	DNA sequence
dsDNA 1	5′-GATGCGFGCGCGCGACTGAC-3′ 3′-CTACGCGCGCGCGCTGAFTG-5′
dsDNA 2	5′-GCGFA**TTGTGAGCGGATAACAATT**TGGCG-3′ 3′-CGCGT**AACACTCGCCTATTGTTAA**AFCGC-5′

The abasic sites are denoted by F. The bold sequence in dsDNA 2 is the 19-mer Lac repressor consensus sequence.

Electrophoretic mobility shift assay

Aliquots of LacI from *Escherichia coli* (150 μM) in MES buffer (MES 20 mM pH 6.0, NaCl 300 mM, 50% in ^2H_2O) were prepared. ^{32}P-labeled 29-mer dsDNA (50 nM) was incubated for 20 min at room temperature with two equivalents of **ç** spin label and Lac repressor, titrated at 0.25, 0.5, 0.75, 1.25, 2.5, 5 and 12.5 μM, in MES buffer (MES 20 mM pH 6.0, NaCl 300 mM, 100% in ^2H_2O), before loading onto 12% native acrylamide gel (90 mM Tris-borate, 2 mM EDTA). Gels were run at 130 V for 4 h, exposed to phosphor imaging screen and visualized using a Fuji FLA5000 imager.

Preparation of dsDNA 2 with lac repressor

29-Mer DNA oligomers (4 nmol) were mixed with two equivalents of **ç** dissolved in ethanol (8 nmol) and annealed in phosphate buffer (Na_2HPO_4 10 mM, NaCl 100 mM, Na_2EDTA 0.1 mM, pH 7.00) (100 μl). The solvent was removed under vacuum, and the dry sample was dissolved in MES buffer (MES 20 mM pH 6.0, NaCl 300 mM, 50% in ^2H_2O) containing Lac repressor (315 μM) (80 μl) and deuterated ethylene glycol (20 μl). The sample was transferred to an EPR tube and rapidly frozen in a freezing mixture ~10 min after addition of LacI. The sample was stored in liquid nitrogen.

Preparation of dsDNA 3

29-Mer DNA oligomers (4 nmol) spin labeled with the **Ç** spin label were annealed in phosphate buffer (Na_2HPO_4 10 mM, NaCl 100 mM, Na_2EDTA 0.1 mM, pH 7.00) (100 μl). The solvent was removed under vacuum, and the dry sample was dissolved in MES buffer (MES 20 mM pH 6.0, NaCl 300 mM, in ^2H_2O) (80 μl) and deuterated ethylene glycol (20 μl). The sample was transferred to an EPR tube, rapidly frozen in a freezing mixture and stored in liquid nitrogen.

Preparation of dsDNA 3 with lac repressor

29-Mer DNA oligomers (4 nmol) spin labeled with the **Ç** spin label were annealed in phosphate buffer (Na_2HPO_4 10 mM, NaCl 100 mM, Na_2EDTA 0.1 mM, pH 7.00) (100 μl). The solvent was removed under vacuum, and the dry sample was dissolved in MES buffer (MES 20 mM pH 6.0, NaCl 300 mM, 50% in ^2H_2O) containing Lac repressor (315 μM) (80 μl) and deuterated ethylene glycol (20 μl). The sample was transferred to an EPR tube and rapidly frozen in a freezing mixture ~10 min. after addition of LacI. The sample was stored in liquid nitrogen.

Pulse EPR measurements

Pulse EPR measurements were done using a Bruker ELEXSYS E580 X-band EPR spectrometer with a standard flex line probe head, housing a dielectric ring resonator (MD4). For measurements at cryogenic temperatures, a continuous-flow helium cryostat (CF935) and a temperature control system (ITC 502) from Oxford instruments were used. All pulsed experiments were performed at 50 K. For PELDOR measurements, a double-microwave frequency setup available from Bruker was used. Microwave pulses were amplified with a TWT amplifier (117X) from Applied Systems Engineering. PELDOR experiments were done using the four-pulse sequence, $\pi/2(\nu_A) - \tau_1 - \pi(\nu_A) - (\tau_1 + t) - \pi(\nu_B) - (\tau_2 - t) - \pi(\nu_A) - \tau_2 -$ echo. To eliminate receiver offsets, the $\pi/2(\nu_A)$ pulse was phase cycled by applying the microwave pulse consecutively through the $+<x>$ and $-<x>$ channels and subtracting the signals. The length of the detection pulses (ν_A) were set to 16 ($\pi/2$) and 32 ns (π). The frequency of the inversion pulse (ν_B) was set at the maximum of the nitroxide field sweep spectrum, and the length was set to 16 ns. Amplitude and phase of the pulses were set to optimize the refocused echo (RE). The frequency of the detection pulses (ν_A) was 40–90 MHz higher than the frequency of the inversion pulse (ν_B). All PELDOR spectra were recorded with a short repetition time of 4000–5000 μs, video amplifier bandwidth of 20 MHz and amplifier gain of 51–57 dB. τ_1 was set to 200 ns for samples in protonated matrix and to 380 ns for samples in deuterated matrix. Proton and deuterium modulation were suppressed by incrementing τ_1 by 8 ns eight times and adding the consecutive spectra. The time increment of the inversion pulse was set to either 12 or 30 ns.

Data analysis, simulation and modeling

Experimental PELDOR time traces were background subtracted and Fourier transformed using DeerAnalysis2011 (16). Distance distributions were generated from orientation average time traces using Tikhonov regularization, as implemented in DeerAnalysis2011. The equilibrium geometry of spin label **ç** was calculated using density functional theory (DFT) with the B3LYP functional and 6-31 G* basis set as implemented in Spartan (Wavefunction). B-form DNA structures were modeled with the make-na server from http://casegroup.rutgers.edu/Biomer/index.html. Abasic sites were introduced into the DNA duplexes by deleting the corresponding cytosine and replacing the glycosidic bond with hydrogen using PyMol (DeLano Scientific LLC). Simulated PELDOR time traces and distance distributions were done using a Matlab program as previously described (17).

RESULTS AND DISCUSSIONS

Sequence-specific binding of DNA by proteins regulates transcription and translation processes and thereby

expression of specific genes. Such binding events have been studied by several techniques, such as foot printing (18), photochemical cross-linking (19) and various spectroscopic approaches (20). There are a number of examples of major conformational changes associated with such binding events (21,22). Studying the details of such molecular rearrangements requires high-resolution techniques, such as X-ray crystallography (23) or NMR spectroscopy (24,25). Unfortunately high-resolution structures of nucleic acid/protein complexes are not readily obtained, and static crystal structures give limited information about dynamics that may play a role in the mechanism of gene regulation (26). Solution studies through long-range distance measurements have been performed using fluorescence resonance energy transfer (FRET), but this technique suffers from the flexibility and uncertainty in orientation of the dyes (27). On the other hand, the use of rigid spin labels and PELDOR enables accurate distance measurements and also yields information on orientations (14).

The PELDOR method

PELDOR can determine distances between two nitroxide spin labels, placed into biopolymers using SDSL (28), through measurement of the dipolar coupling between the two spins. The relationship between dipolar coupling and distance is described by Equation (1) (29):

$$\nu_{\mathrm{dip}} = \frac{52.16}{r^3}\left(1 - 3\cos^2\theta\right), \qquad (1)$$

where 52.16 is the dipolar splitting constant for two nitroxides, r is the magnitude of the interspin distance vector **r** and θ is the angle between the applied magnetic field B_0 and the distance vector. In a four-pulse PELDOR experiment, the intensity of the RE, created from spins in resonance with the detection sequence ν_A (spins A), is modulated by the inversion of spins in resonance with the inversion pulse ν_B (spins B) (Figure 2). The frequency of this modulation is the dipolar coupling between spins A and B. When the orientation of the spin centers in a molecule is fixed, the modulation frequency and depth of the PELDOR time trace become dependent on the frequency of the detection sequence (9).

PELDOR measurements on dsDNA 1

dsDNA 1 was mixed with two equivalents of the spin label **ç** and then hybridized in phosphate buffer containing 20% ethylene glycol as cryoprotectant. Binding of the spin labels to the abasic sites was confirmed by measuring the noncovalently spin-labeled DNA with continuous wave (CW) EPR at 0 to −40°C (Supplementary Information, Supplementary Figure S1). The spin-labeled dsDNA was then measured with four-pulse PELDOR (2), placing the inversion pulse at the center of the nitroxide spectrum and the detection pulse sequence at 40–90 MHz higher frequency (Figure 3). At 90 MHz offset, the detection sequence excites predominantly the A_{zz} component of the ^{14}N hyperfine tensor. Decreasing the frequency offset to 40 MHz results in an increased excitation of A_{xx}, A_{yy} and off-diagonal components.

Acquiring the PELDOR experiments at 40–90 MHz offset, in steps of 10 MHz, resulted in the time traces with varying modulation frequency and depth shown in Figure 4a. The PELDOR time trace acquired at 40 MHz offset has a modulation depth Δ of about 0.16 (Figure 4c). This modulation depth depends on the relative orientation of the spin labels, the degree of orientation correlation, the ratio between coupled spin pairs in DNA and the total spin concentration (30). Therefore, comparing this modulation depth to one of a DNA with the same base sequence but with the covalently attached spin label **Ç** (which is 100% doubly spin-labeled) gives access to the degree of noncovalent binding, assuming that the relative orientation and the orientation correlation are the same. The covalently labeled DNA duplex, at 40 MHz offset, had a modulation depth of about 0.45 (9). Comparing this to the modulation depth of 0.16 for the noncovalently labeled DNA indicates that 0.16/0.45 = 36% of the DNA duplexes contain two noncovalently bound spin labels. The same result was obtained at the other frequency offset. The percentage of doubly labeled DNAs could not be increased by increasing the ratio of spin label to duplex nor by varying the flanking bases for both abasic sites (31). Rapidly freezing the noncovalently spin-labeled DNA either before or after cooling the sample to approximately −30°C did not affect the modulation depth (data not shown).

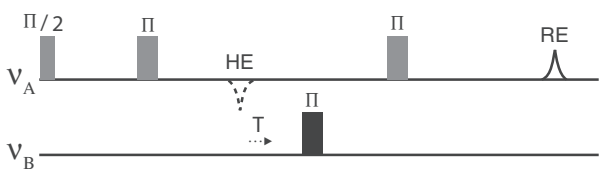

Figure 2. The four-pulse PELDOR sequence. The detection sequence ν_A is in gray. The inversion pulse ν_B is in black. The Hahn echo (HE) and RE are denoted by a broken and solid line, respectively.

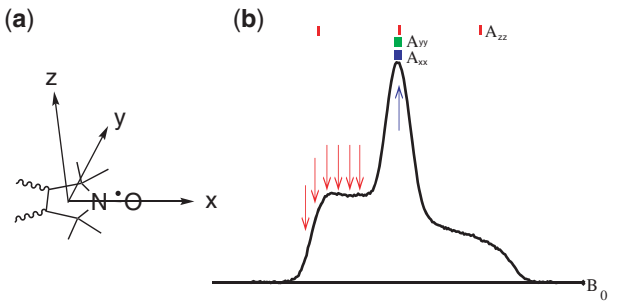

Figure 3. The A-tensor frame and EPR spectrum for a nitroxide. (**a**) A nitroxide and the relative orientation of the A-tensor's principal components. (**b**) A nitroxide EPR spectrum at X-band. The blue arrow indicates the position of the inversion pulse. The red arrows indicate the position of the detection pulses at 40–90 MHz offsets between the frequencies of the detection and inversion pulses. The sticks at the top of the figure show the approximate positions of the ^{14}N hyperfine coupling components.

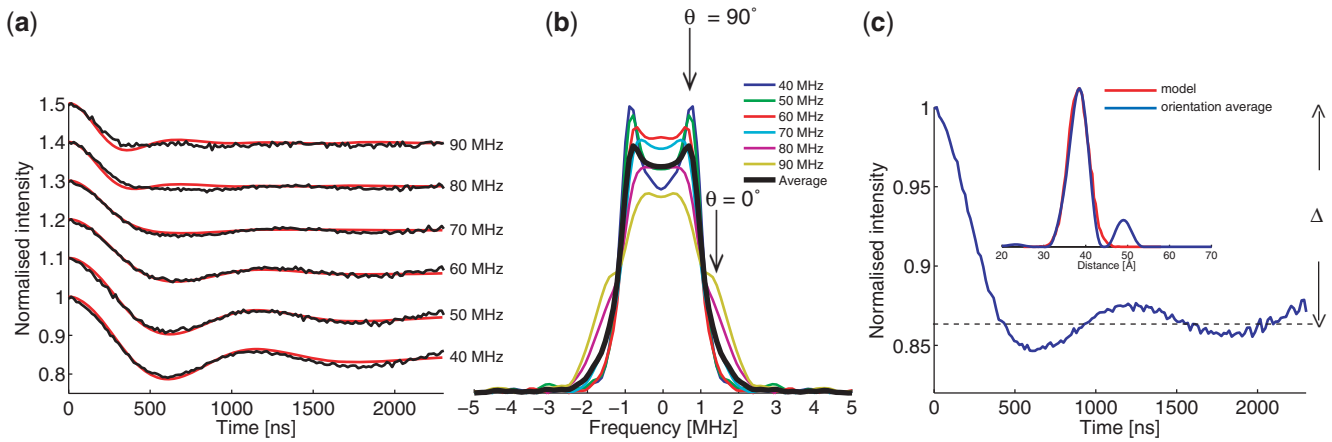

Figure 4. PELDOR data for **dsDNA 1**. (**a**) PELDOR time traces of noncovalently spin-labeled **dsDNA 1** (black) with simulated time traces overlaid (red). The time traces have been background subtracted, normalized and displaced on the *y*-axis for clarity (original time traces are depicted in the Supplementary Information). (**b**) Fourier transformation of the experimental time traces and their sum. Arrows point to the perpendicular and parallel components. (**c**) Orientation-averaged time trace and distance distribution from simulation (red) and summed time trace (blue). Δ represents the modulation depth.

The dependence of the dipolar frequency on the frequency offset can be seen in the Fourier transformed time traces in Figure 4b. These show that the parallel component of the dipolar spectrum ($\theta = 0^{\circ}$) increases in intensity as the detection sequence is moved from 40 to 90 MHz offset. This trend was also observed for the covalently spin labeled dsDNA (9) and indicates that the A_{zz} components of the rigid spin label **ç** are approximately parallel to the interspin vector **r** (Figure 5a). Since the PELDOR time traces of the noncovalently spin-labeled dsDNA show that the spin-label orientation is correlated with the orientation of the interspin vector **r**, the distance distribution cannot be obtained from the individual time traces using the program DeerAnalysis2011 (32). Instead, all six time traces recorded at the different spectral positions were added together, as described by Godt *et al.* (33), which yields an orientation-averaged time trace. The resulting orientation-averaged time trace, its Fourier transformation and the corresponding distance distribution are shown in Figure 4b and c. The obtained distance distribution has a mean distance of 38 ± 2.2 Å (Figure 4c, inset), nearly identical to that previously determined for the covalently spin-labeled **dsDNA 1** (37 ± 1 Å) (9).

To obtain information on the conformational dynamics of the dsDNA and spin label orientation, the PELDOR time traces were simulated with an in-house Matlab® program (17) using the cooperative twist-stretch dynamic model for short dsDNA (34,35) (Supplementary Figure S2) that was recently applied by the lab of Prisner (14) for the analysis of PELDOR data obtained from the covalent version of our label. Using identical dynamics parameters as for the covalently spin labeled dsDNA (14), except for the mean distance (see Supplementary Information, Supplementary Table S1), the simulated PELDOR time traces agree well with the experimental time traces (Figure 4a) and yield a distance distribution in agreement with the distribution from the orientation-averaged time trace (Figure 4c). It should also be noted that all six time traces were simulated with the same set of geometrical parameters. Interspin distances obtained from PELDOR, simulations and modeling DNA duplexes are summarized in Table 2.

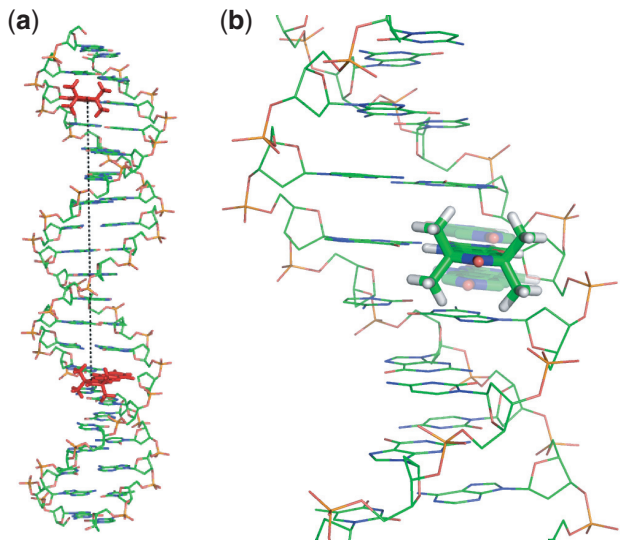

Figure 5. Molecular models of the noncovalently spin-labeled **dsDNA 1**. (**a**) Molecular model of **dsDNA 1** showing the relative positioning of the **ç** spin labels (red) and the distance vector between them (broken black line). (**b**) A close-up view of **ç** (stick representation) within the DNA abasic site. The conformational dynamics of the spin label, as implemented in the PELDOR simulations, are depicted. The transparent spin labels show how the spin labels move away from an equilibrium position upon cooperative twist-stretching of the DNA helix. The conformational dynamics of the DNA helix have been omitted, and the methyl groups of the transparent spin labels have been removed for clarity.

Observing LacI-induced DNA bending by PELDOR

To assess the applicability of noncovalent spin labeling for distance measurements on DNA/protein complexes, the

binding of the Lac repressor protein (LacI) to the consensus Lac operator DNA sequence (Figure 6) was chosen as a proof of principle experiment. The Lac repressor binds specifically to the operator and distorts the DNA from its B-form by bending the center of the operator sequence through an angle of ~45° (37–39). If the LacI protein is able to bind to a DNA containing two abasic sites occupied by the spin label **ç**, then the accompanied bending of the DNA should manifest in a distance change in the PELDOR experiment.

For this experiment, we used a 29-mer dsDNA that contains a 19-mer Lac consensus sequence and two abasic sites (**dsDNA 2,** Table 1). To verify the binding of the Lac repressor protein (LacI from *Escherichia coli*) to the dsDNA, an electrophoretic mobility shift assay was used. The 29 base pair DNA duplex with two abasic sites was radiolabeled with ^{32}P and 50 nM duplex incubated with an increasing concentration of LacI before electrophoresis and imaging. A clear shift of the DNA upon protein binding was observed, yielding an apparent dissociation constant of ~1 μM LacI (Figure 7). This suggests that the protein is fully bound at the concentrations used for EPR experiments. Similar results were obtained whether or not the spin label **ç** was present. The binding affinity is weaker than that published previously for the Lac repressor using membrane filtering (40), most likely due to the relatively short length of DNA used, the incorporation of two abasic sites and the use of the gel-shift technique, which tends to underestimate binding affinity due to extended incubation times.

Table 2. Interspin distances for all dsDNA

dsDNA	r_{DA}[a] (Å)	$r_{Simulation}$[b] (Å)	$r_{MM/X\text{-}ray}$[c] (Å)
dsDNA 1	38.0 ± 2.2	38.6 ± 2.5 (0.4 ± 0.1)	38
dsDNA 2	69.2 ± 3.8	70.0 ± 4.8 (1 ± 0.1)	73
dsDNA 2 + LacI	64.6 ± 4.1	65.0 ± 5.3 (1 ± 0.1)	67

[a]Most probable distance ± one standard deviation from orientation-averaged PELDOR time traces using DeerAnalysis 2011.
[b]Most probable distance ± one standard deviation. The error in the distance ± one standard deviation is in brackets.
[c]Interspin distances obtained from molecular modeling using B-form DNA duplexes. The interspin distance for **dsDNA 2** bound to LacI was estimated by modeling spin labels into the X-ray structure of a 21-mer dsDNA bound to LacI (pdb id. 1LBG).

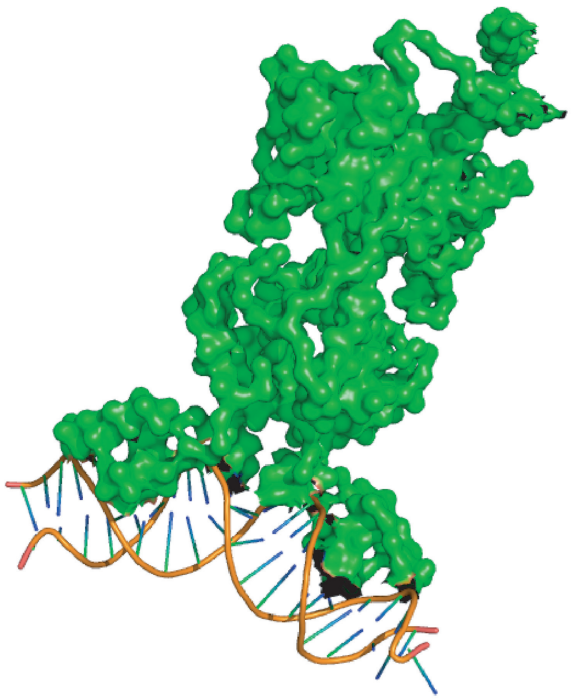

Figure 6. Lac repressor dimer bound to a 21-mer symmetric Lac operator (PDB 1LBG) (36). The Lac repressor is represented in surface mode. The Lac operator DNA is represented in cartoon mode.

The **dsDNA 2** was noncovalently spin labeled with two equivalents of spin label **ç** and measured with PELDOR at 40–90 MHz frequency offsets, both before and after addition of LacI. The PELDOR time trace of the DNA duplex alone at 40 MHz has a modulation depth of 0.2 (Figure 8a), corresponding to ~40% doubly spin-labeled duplex DNA. This is comparable to the binding observed for **dsDNA 1**, taking into account the error in determining the modulation depth and different label orientation. The change in the modulation period for **dsDNA 2** is not as visible as for **dsDNA 1** (Figure 8a and b) but increasing the frequency offset from 40 to 90 MHz leads to a decrease in modulation depth. The Fourier transformations of the individual time traces show less pronounced orientation selection for this DNA (Figure 8c and d). This could be due to the increased interspin distance and flexibility or that the angle between the interspin vector and the *z* component of the spin labels' ^{14}N hyperfine coupling tensor (A_{zz}) is around 45° (9). To observe at least one full period of the dipolar modulation, the time window had to be extended to 7 μs. This considerably reduces the monitored echo intensity and results in a time trace with worse signal to noise than for **dsDNA 1**.

The distance distribution from the orientation-averaged PELDOR time trace has a mean distance of 69.2 Å (Figure 8e, inset), close to the mean distance of 68.1 Å

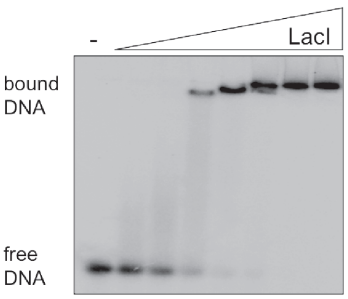

Figure 7. Electrophoretic mobility shift assay showing binding of the Lac repressor to the **dsDNA 2** in the presence of the spin label **ç**. DNA (50 nM) was titrated with 0, 0.25, 0.5, 0.75, 1.25, 2.5, 5 and 12.5 μM LacI dimer before separation by gel electrophoresis and gel visualization. An apparent dissociation constant of ~1 μM was observed. The second, more retarded species observed at high protein concentrations is likely due to the known propensity for LacI to tetramerise.

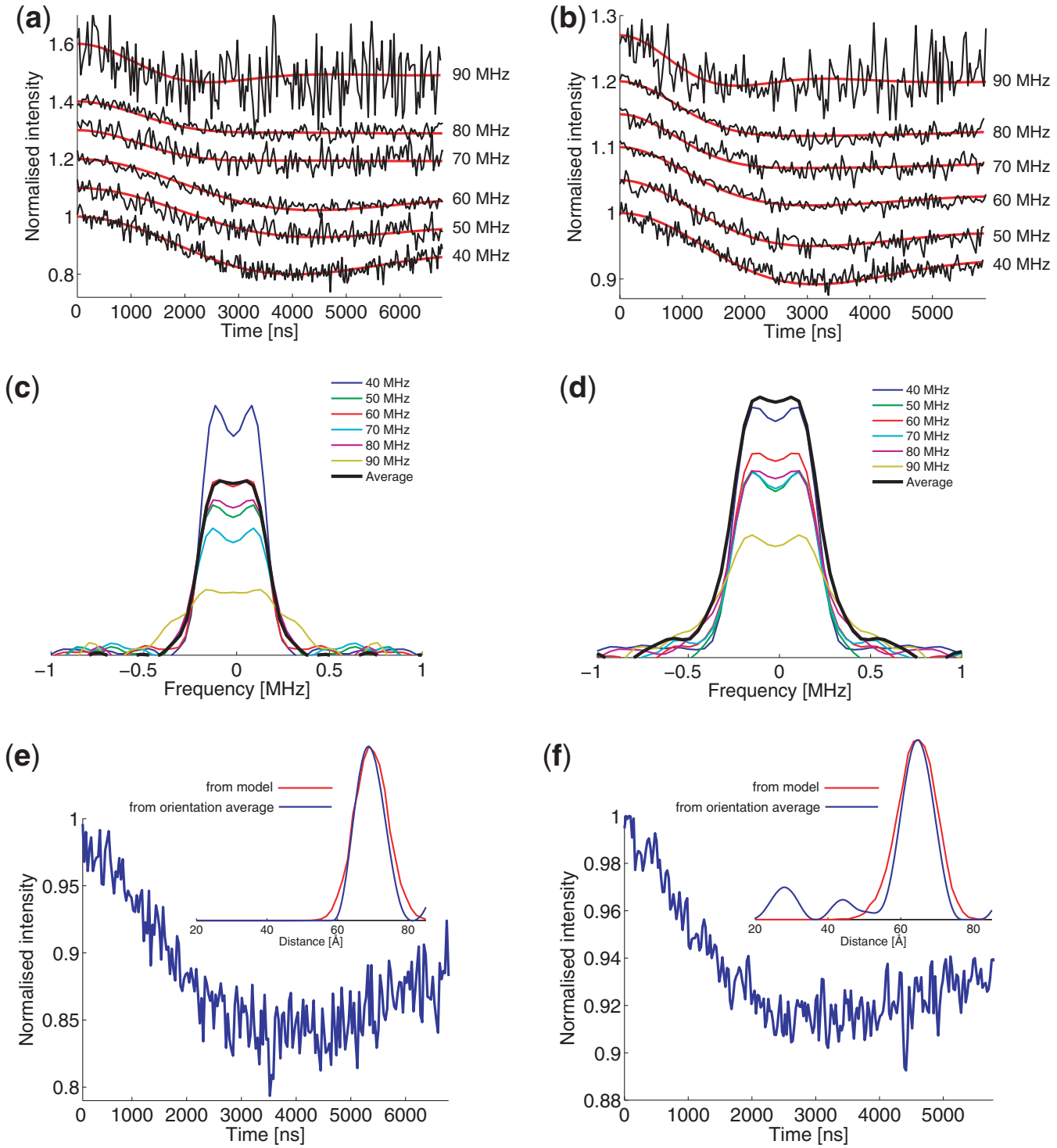

Figure 8. PELDOR data for noncovalently spin-labeled **dsDNA 2** with and without LacI at 40–90 MHz offsets. (**a**) and (**b**) Background-corrected PELDOR time traces of **dsDNA 2** without and with LacI (black), respectively, overlaid with the corresponding simulated time traces (red). The time traces have been displaced on the *y*-axis for clarity. Original time traces are shown in the Supplementary Information, Supplementary Figure S5. (**c**) and (**d**) are the respective Fourier transformations of the time traces in (a) and (b). The black spectra are the Fourier transformations of the respective summed time traces shown in (**e**) and (**f**). (e) and (f) are the summed PELDOR time traces of **dsDNA 2** without and with LacI, respectively. The inset shows the distance distribution obtained from the summed time traces using DeerAnalysis (blue) and the distribution obtained from model-based simulations.

obtained from PELDOR measurements on an identical DNA duplex covalently spin labeled with **Ç** (Supplementary Information, Supplementary Figure S3 and Supplementary Table S2, S3). Simulations of the PELDOR time traces for **dsDNA 2** using the cooperative twist-stretch dynamics model (14) yields a distance distribution with a mean distance of 70 Å (Figure 8e, inset), which is in good agreement with the result from DeerAnalysis. The

PELDOR time traces for **dsDNA 2** bound to the Lac repressor show a modulation but only a weakly resolved orientation selection (Figure 8b and d). The modulation depth at 40 MHz of 0.1 indicates that 20% of the dsDNA are doubly labeled. The decrease in noncovalent spin labeling efficiency is attributed to deformation of the DNA and abasic sites due to LacI binding, which impedes spin-label binding into the abasic sites. However, the labeling efficiency and specificity are still large enough to yield modulated PELDOR time traces. The distance distribution from the orientation-averaged time trace has a mean distance of 64.6 Å (Figure 8f, inset). Comparing the orientation-averaged PELDOR time traces and distance distributions for **dsDNA 2** and **dsDNA 2 + LacI** clearly shows the change in interspin distance upon binding of LacI (Figure 9).

Using the mean distances obtained from the orientation-averaged PELDOR time traces for the bound and unbound duplexes and trigonometry (41) yields a bending angle of 42°, which is in good agreement with a bending angle of ~45° observed from crystal structure (39) and the 48.5° obtained from PELDOR measurements on the covalently spin-labeled DNA (Supplementary Information, Supplementary Figure S4). Although the change in the observed interspin distance corresponds nicely to a 42° bending of the DNA, this approach does not take into account the fact that the spin labels stick out from the DNA helix and change their relative orientation when LacI bends the DNA. Furthermore, addition of time traces acquired at discrete field positions does not represent a complete orientation-averaged time trace (42). This motivated us to simulate the PELDOR time traces of the DNA/LacI complex using a model with the twist-stretch dynamics of the unbound DNA. Assuming that LacI bends the operator DNA symmetrically around the central base pair, which is valid according to the X-ray structure, and using simple trigonometry, it can be estimated that a 42° bending of the DNA should decrease the distance between the two abasic sites by about 4.6 Å and tilt each spin label ~21° toward the interspin vector (Figure 10). Furthermore, to obtain a good fit to the experimental modulation frequency, it was necessary to increase the equilibrium angle between the N-O axes of the spin labels (torsion angle) by 15°, relative to the angle used for the unbound DNA. This change in the torsion angle can be rationalized by the unwinding of the DNA upon binding to LacI (36). These geometric parameters were then combined with the twist/stretch dynamics model used for the **dsDNA 2**. The geometric and dynamics parameters that resulted in simulations with a good fit to the experimental time traces (Figure 8b) are listed in Supplementary Table S1. These parameters yield a distance distribution with a mean distance of 65 Å, which fits nicely to the distance obtained from DeerAnalysis (Table 2).

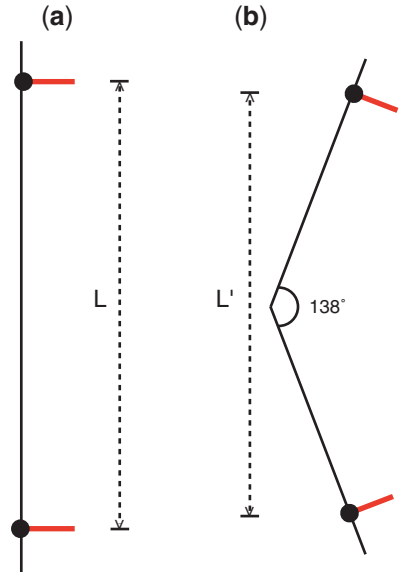

Figure 10. Diagram illustrating the change in distance between the DNA abasic sites and spin-label orientation upon DNA bending. The **dsDNA 2** is represented by black solid lines, abasic sites by black circles and spin labels by red lines. (**a**) Unbound **dsDNA 2**. The distance between the abasic sites (the height between spin labels) is denoted by *L*. (**b**) **dsDNA 2** after being bent 42° about the center by the LacI protein. The distance between the abasic site, which now has become shorter, is denoted by *L*'.

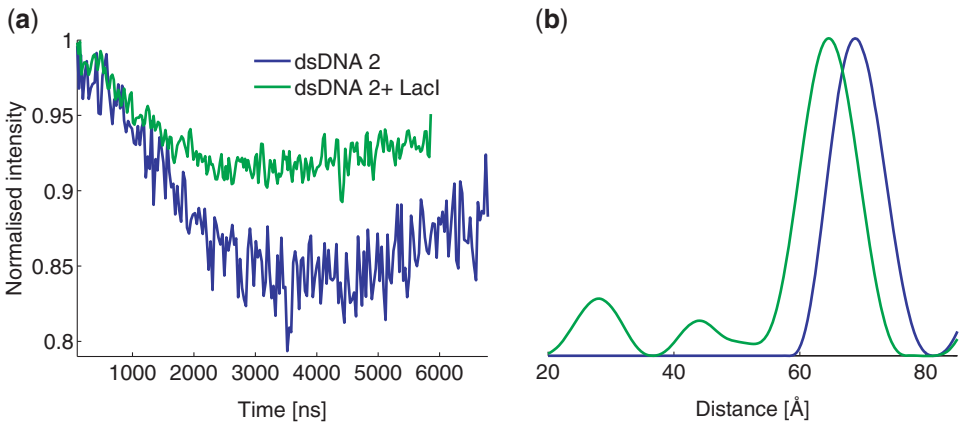

Figure 9. Overlay of the PELDOR data for **dsDNA 2** and **dsDNA 2 + LacI**. (**a**) Background-corrected orientation-averaged time traces. (**b**) Distance distributions from the time traces in (a) obtained by Tikhonov regularization.

CONCLUSIONS

We have noncovalently spin-labeled dsDNA with the rigid spin label **ç** and used PELDOR to measure the interspin distance, label orientations and conformational dynamics of DNA duplexes and a DNA/protein complex. We were able to show that the LacI protein binds and bends DNA in the presence of noncovalently bound spin labels. The protein does displace a fraction of the labels but are still bound to enable PELDOR measurements. Measuring this DNA/protein complex enabled us to evaluate the limits for the noncovalent spin labeling method to be close to 70 Å for the maximum distance, 20% for the double spin labeling efficiency and 4.5 Å as a detectable distance change. We have obtained PELDOR time traces that show clear modulation and orientation selectivity. Most importantly, the noncovalent but site-directed labeling strategy, with the rigid spin label **ç**, simply requires mixing spin label and DNA, followed by PELDOR measurements. Since DNA strands containing abasic sites at specific sites are commercially available, this strategy is widely applicable and should facilitate dissemination of this EPR methodology.

SUPPLEMENTARY DATA

Supplementary Data are available at NAR Online: Supplementary Tables 1–3, Supplementary Figures 1–5 and Supplementary Information.

ACKNOWLEDGEMENTS

The authors thank Biljana Petrovic-Stojanovska, BSRC, University of St Andrews, for preparing the LacI protein.

FUNDING

Biotechnology and Biological Sciences Research Council [BB/H017917/1]; Engineering and Physical Sciences Research Council [F004583/1]; Icelandic Research Fund [110035021]; Scottish Overseas Research Students (SORS) Scholarship from the School of Biology, University of St Andrews (to G.W.R.); Doctoral fellowship from the University of Iceland Research Fund (to S.A.S.); Research Councils of the UK for an RCUK fellowship (to O.S.). Funding for open access charge: Wellcome Trust [091825/Z/10/Z].

Conflict of interest statement. None declared.

REFERENCES

1. Milov,A.D., Salikhov,K.M. and Shirov,M.D. (1981) Application of the double resonance method to electron spin echo in a study of the spatial distribution of paramagnetic centers in solids. *Soviet Phys Solid State*, **23**, 565–569.
2. Martin,R., Pannier,M., Diederich,F., Gramlich,V., Hubrich,M. and Spiess,H. (1998) Determination of end-to-end distances in a series of TEMPO diradicals of up to 2.8 nm length with a new four-pulse double electron electron resonance experiment. *Angew. Chem. Int. Ed.*, **37**, 2833–2837.
3. Zhang,X., Cekan,P., Sigurdsson,S.T. and Qin,P. (2009) Studying RNA using site-directed spin-labeling and continuous-wave electron paramagnetic resonance spectroscopy. *Methods Enzymol.*, **469**, 303–328.
4. Klare,J.P. and Steinhoff,H.-J. (2009) Spin labeling EPR. *Photosynth. Res.* **102**, 377–390.
5. Shelke,S.A. and Sigurdsson,S.T. (2012) Site-directed spin labelling of nucleic acids. *Eur. J. Org. Chem.*, **2012**, 2291–2301.
6. Schiemann,O. and Prisner,T.F. (2007) Long-range distance determinations in biomacromolecules by EPR spectroscopy. *Q. Rev. Biophys.*, **40**, 1–53.
7. Griffith,O.H. and Waggoner,A.S. (1969) Nitroxide free radicals: spin labels for probing biomolecular structure. *Acc. Chem. Res.*, **2**, 17–24.
8. Miller,T.R., Alley,S.C., Reese,A.W., Solomon,M.S., McCallister,W.V., Mailer,C., Robinson,B.H. and Hopkins,P.B. (1995) A probe for sequence-dependent nucleic acid dynamics. *J. Am. Chem. Soc*, **117**, 9377–9378.
9. Schiemann,O., Cekan,P., Margraf,D., Prisner,T.F. and Sigurdsson,S.T. (2009) Relative orientation of rigid nitroxides by PELDOR: beyond distance measurements in nucleic acids. *Angew. Chem. Int. Ed.*, **48**, 3292–3295.
10. Barhate,N., Cekan,P., Massey,A. and Sigurdsson,S. (2007) A nucleoside that contains a rigid nitroxide spin label: a fluorophore in disguise. *Angew. Chem. Int. Ed.*, **46**, 2655–2658.
11. Cekan,P., Smith,A.L., Barhate,N., Robinson,B.H. and Sigurdsson,S.T. (2008) Rigid spin-labeled nucleoside Ç: a nonperturbing EPR probe of nucleic acid conformation. *Nucleic Acids Res.*, **36**, 5946–5954.
12. Smith,A.L., Cekan,P., Brewood,G.P., Okonogi,T.M., Alemayehu,S., Hustedt,E.J., Benight,A.S., Sigurdsson,S.T. and Robinson,B.H. (2009) Conformational equilibria of bulged sites in duplex DNA studied by EPR spectroscopy. *J. Phys. Chem. B*, **113**, 2664–2675.
13. Cekan,P., Jonsson,E.Ö. and Sigurdsson,S.T. (2009) Folding of the cocaine aptamer studied by EPR and fluorescence spectroscopies using the bifunctional spectroscopic probe C. *Nucleic Acids Res.*, **37**, 3990–3995.
14. Marko,A., Denysenkov,V., Margraf,D., Cekan,P., Schiemann,O., Sigurdsson,S.T. and Prisner,T.F. (2011) Conformational flexibility of DNA. *J. Am. Chem. Soc.*, **133**, 13375–13379.
15. Shelke,S.A. and Sigurdsson,S.T. (2010) Noncovalent and site-directed spin labeling of nucleic acids. *Angew. Chem. Int. Ed.*, **49**, 7984–7986.
16. Jeschke,G., Chechik,V., Ionita,P., Godt,A., Zimmermann,H., Banham,J., Timmel,C.R., Hilger,D. and Jung,H. (2006) DeerAnalysis2006—a comprehensive software package for analyzing pulsed ELDOR data. *Appl. Magn. Reson.*, **30**, 473–498.
17. Reginsson,G.W., Hunter,R.I., Cruickshank,P.A.S., Bolton,D.R., Sigurdsson,S.T., Smith,G.M. and Schiemann,O. (2012) W-band PELDOR with 1kW microwave power: molecular geometry, flexibility and exchange coupling. *J. Magn. Reson.*, **216**, 175–182.
18. Galas,D.J. and Schmitz,A. (1978) DNAase footprinting: a simple method for the detection of protein-DNA binding specificity. *Nucleic Acids Res.*, **5**, 3157–3170.
19. Welsh,J. and Cantor,C.R. (1984) Protein–DNA cross-linking. *Trends Biochem. Sci.*, **9**, 505–508.
20. Lohman,T.M. and Bujalowski,W. (1991) Thermodynamic methods for model-independent determination of equilibrium binding isotherms for protein-DNA interactions: spectroscopic approaches to monitor binding. *Methods Enzymol.*, **208**, 258–290.
21. Rhodes,D., Schwabe,J.W.R., Chapman,L. and Fairall,L. (1996) Towards an understanding of protein-DNA recognition. *Philos. Trans. Roy Soc. B: Biol. Sci.*, **351**, 501–509.
22. Luscombe,N.M., Austin,S.E., Berman,H.M. and Thornton,J.M. (2000) An overview of the structures of protein-DNA complexes. *Genome Biol.*, **1**, 001.1–001.10.
23. Frederick,C.A., Grable,J., Melia,M., Samudzi,C., Jen-Jacobson,L., Wang,B.-C., Greene,P., Boyer,H.W. and Rosenberg,J.M. (1984) Kinked DNA in crystalline complex with EcoRI endonuclease. *Nature*, **309**, 327–331.
24. Prestegard,J.H., Al-Hashimi,H.M. and Tolman,J.R. (2000) NMR structures of biomolecules using field oriented media and residual dipolar couplings. *Q. Rev. Biophys.*, **33**, 371–424.
25. Renault,M., Cukkemane,A. and Baldus,M. (2010) Solid-state NMR spectroscopy on complex biomolecules. *Angew. Chem. Int. Ed.*, **49**, 8346–8357.

26. Langowski,J., Benight,A.S., Fujimoto,B.S., Schurr,J.M. and Schomburg,U. (1985) Change of conformation and internal dynamics of supercoiled DNA upon binding of Escherichia coli single-strand binding protein. *Biochemistry*, **24**, 4022–4028.
27. Hillisch,A., Lorenz,M. and Diekmann,S. (2001) Recent advances in FRET: distance determination in protein–DNA complexes. *Curr. Opin. Struct. Biol.*, **11**, 201–207.
28. Steinhoff,H. (2004) Inter-and intra-molecular distances determined by EPR spectroscopy and site-directed spin labeling reveal protein-protein and protein-oligonucleotide interaction. *Biol. Chem.*, **385**, 913–920.
29. Slichter,C.P. (1990) *Principles of Magnetic Resonance*, 3rd edn. Springer, Heidelberg, Germany.
30. Bode,B.E., Margraf,D., Plackmeyer,J., Dürner,G., Prisner,T.F. and Schiemann,O. (2008) Counting the monomers in nanometer-sized oligomers by pulsed electron−electron double resonance. *J. Am. Chem. Soc.*, **129**, 6736–6745.
31. Shelke,S.A. and Sigurdsson,S.T. (2011) Structural changes of an abasic site in duplex DNA affect noncovalent binding of the spin label c. *Nucleic Acids Res.*, **40**, 3732–3740.
32. Jeschke,G. and Polyhach,Y. (2007) Distance measurements on spin-labelled biomacromolecules by pulsed electron paramagnetic resonance. *Phys. Chem. Chem. Phys.*, **9**, 1895–1910.
33. Godt,A., Schulte,M., Zimmermann,H. and Jeschke,G. (2006) How flexible are poly (paraphenyleneethynylene)s? *Angew. Chem. Int. Ed.*, **45**, 7560–7564.
34. Gore,J., Bryant,Z., Nöllmann,M., Le,M.U., Cozzarelli,N.R. and Bustamante,C. (2006) DNA overwinds when stretched. *Nature*, **442**, 836–839.
35. Marko,J. (1997) Stretching must twist DNA. *Europhys. Lett.*, **38**, 183–188.
36. Lewis,M., Chang,G., Horton,N.C., Kercher,M.A., Pace,H.C., Schumacher,M.A., Brennan,R.G. and Lu,P. (1996) Crystal structure of the lactose operon repressor and its complexes with DNA and inducer. *Science*, **271**, 1247–1254.
37. Bahl,C.P., Wu,R., Stawinsky,J. and Narang,S.A. (1977) Minimal length of the lactose operator sequence for the specific recognition by the lactose repressor. *Proc. Natl Acad. Sci. USA*, **74**, 966–970.
38. Bell,C. and Lewis,M. (2000) A closer view of the conformation of the Lac repressor bound to operator. *Nat. Struct. Mol. Biol.*, **7**, 209–214.
39. Lewis,M. (2005) The lac repressor. *C. R. Biol.*, **328**, 521–548.
40. Riggs,A.D., Suzuki,H. and Bourgeois,S. (1970) lac repressor-operator interaction. *J. Mol. Biol.*, **48**, 67–83.
41. Kuznetsov,N.A., Milov,A.D., Koval,V.V., Samoilova,R.I., Grishin,Y.A., Knorre,D.G., Tsvetkov,Y.D., Fedorova,O.S. and Dzuba,S. (2009) PELDOR study of conformations of double-spin-labeled single-and double-stranded DNA with non-nucleotide inserts. *Phys. Chem. Chem. Phys.*, **11**, 6826–6832.
42. Jeschke,G. (2012) Interpretation of dipolar EPR data in terms of protein structure. In: *Structure and Bonding*, Springer-Verlag Berlin Heidelberg, Germany. pp.1–38.